

# Mechanochemical Treatment of Waste Poly (Vinyl Chloride) for Alcohol Halogenation by Ball Milling and Triboelectric Material

Du Chen,<sup>1</sup> Shengming Li,<sup>2</sup> Ziye Ren,<sup>1</sup> Chenyu Wang,<sup>1</sup> Ran Ding,<sup>1</sup> Jinxing Chen<sup>2,\*</sup> and Zhao Wang<sup>1,\*</sup>

<sup>1</sup>State and Local Joint Engineering Laboratory for Novel Functional Polymeric Materials, Jiangsu Key Laboratory of Advanced Functional Polymer Materials, Suzhou Key Laboratory of Macromolecular Design and Precision Synthesis, College of Chemistry, Chemical Engineering and Materials Science, Soochow University, Suzhou 215123, China

<sup>2</sup>Institute of Functional Nano & Soft Materials (FUNSOM), Jiangsu Key Laboratory for Carbon-Based Functional Materials & Devices, Soochow University, Suzhou 215123, P. R. China

\*Correspondence and requests for materials should be addressed to

E-mail: [chenjinxing@suda.edu.cn](mailto:chenjinxing@suda.edu.cn), [wangzhao@suda.edu.cn](mailto:wangzhao@suda.edu.cn)

## ABSTRACT

Polyvinyl chloride (PVC), one of the most extensively produced polymers, has raised significant environment and public health concerns due to its persistence in ecosystem, long-term accumulation and associated toxicity. The well-established mechanical recycling approach for treating waste PVC often result in polymer degradation and release of hazardous by-products, such as corrosive HCl. We envisage that mechanical recycling in tandem with a halogenation reaction provide a new solution to waste PVC management. Herein, we demonstrated that PVC plastic could serve as chlorination reagents, in combination with triboelectric catalyst, to achieve efficient halogenation of alcohols under ball milling condition. The triboelectric catalyst, TiO<sub>2</sub>, mediates the single electron transfer process that promotes the dehydrochlorination of PVC, thereby enabling the in-situ chlorination of alcohols. This strategy was applicable to a variety of aliphatic and benzylic alcohols, yielding the corresponding organic chlorides in moderate to excellent yields. In particular, the yield of benzyl chloride reached 95% after 4 h of ball milling. Structural analysis confirmed that polymer formed by dehydrochlorination of PVC contained olefin, carbonyl and aromatic structures. Additionally, Cl could be completely removed, and the molecular weight decreased from 65.0 kDa to 4.6 kDa after recycling and reusing PVC five times. This mechanochemical approach was also successfully applied in real plastics applications and scale-up experiments. Overall, this method provides inspiration for using PVC as a chlorine source to initiate chemical reactions through mechanochemical approaches.

## INTRODUCTION

Polyvinyl chloride (PVC) is one of the top five commodity polymers, accounting for 9.6% of global plastic production.<sup>1-3</sup> Despite their enormous utility, PVC waste management has become a global challenge, as common industrial approaches (direct landfill and incineration) lead to plastic accumulation and emission of hazardous by-products in ecosystem. In addition, pyrolysis of PVC presents similar challenges to incineration. While catalytic hydrocracking has been explored for polyolefins recycling, its application to PVC remains limited due to catalyst deactivation caused by chlorine species.<sup>4,5</sup> Therefore, a two-step process involving PVC

dechlorination followed by decomposition have been developed. PVC can be converted into PE-like materials or serve as a chlorine source to facilitate various chemical reactions via electrocatalysis, metal catalysis or thermal catalysis.<sup>6-12</sup> Despite recent advancements, recycling of PVC still demands harsh conditions and the use of costly metal catalyst, which may pose challenges for large-scale implementation within existing industrial systems.

Mechanical recycling, one of the dominant industrial methods for waste plastic management, commonly involves the repurposing of plastics by sorting, grinding and reprocessing. During grinding process, mechanochemical degradation occurs via force induced polymer chain scission. Recent studies on mechanochemical degradation of polyesters and polyolefins have demonstrated significant advantages, including mild, solvent-free operation conditions and scalability.<sup>13-16</sup> Mechanochemical dichlorination of PVC was also accomplished by ball milling treatment.<sup>17-20</sup> However, in most cases, HCl is produced and typically neutralized with excessive amounts of base, raising significant environmental concerns. Contact-electro-catalysis (CE), a unique form of mechanochemical transformation, leverages tribo-electrification between triboelectric material and substrate to mediate single electron transfer (SET) process.<sup>21</sup> Owing to its unique catalytic activity, cheap and readily available triboelectric materials have recently been employed in the degradation of organic pollutants.<sup>22-24</sup>

Herein, we propose that C-Cl bond in PVC can be activated by CE using commercial available TiO<sub>2</sub> to promote efficient tandem dechlorination and alcohol halogenation reactions under ball milling. This mechanochemical approach enables halogenation of alcohols under mild conditions (air atmosphere, solvent-free), avoiding hazardous reagents and delicate operating conditions commonly associated with conventional protocols. This strategy was applicable to a variety of aliphatic and benzylic alcohols to yield corresponding organic chlorides in moderate to excellent yield. In particular, the yield of benzyl chloride reached 95% after 4 h of ball milling. Structural analysis of degraded-PVC (d-PVC) revealed that it can be completely dechlorinated, resulting in a Cl-free polymer containing olefin, carbonyl and aromatic structures. Notably, the molecular weight of the residual Cl-free polymer is remarkably low (4.6 kDa) after 5 cycles. A high yield of benzyl chloride (89%) could also be achieved using a PVC storage bag as Cl source.

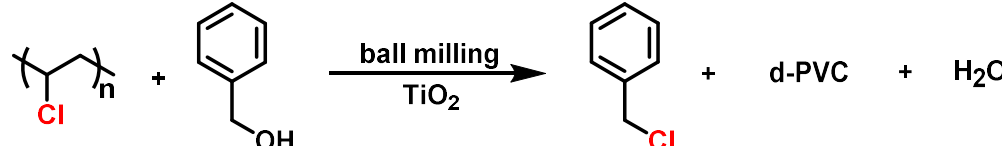
## RESULTS AND DISCUSSION

In this study, we used a commercial PVC ( $M_n=65.0$  kDa) as chlorine source and benzyl alcohol as model substrate for the chlorination of alcohol. Initially, our experiments were conducted in a 10 mL ZrO<sub>2</sub> milling jar with two 10 mm ZrO<sub>2</sub> balls, operating at 30 Hz. The yield of benzyl chloride was determined by gas chromatography mass spectrometry (GC-MS). After 3 hours of ball milling with a 10 wt% TiO<sub>2</sub> loading, a 13% yield of benzyl chloride was observed. Higher TiO<sub>2</sub> loadings resulted in improved yields (Table 1, Entries 1-4), with a maximum yield of 83% at 50 wt% TiO<sub>2</sub> (Table 1, Entry 5). A control experiment without TiO<sub>2</sub> confirmed the significantly lower yield of benzyl chloride (Table 1, Entry 6).

Subsequently, the reaction parameters were further explored by varying the milling frequency and the size of milling balls. It was observed that reducing either the milling frequency or the size of the milling balls resulted in lower yields (Table 1, Entry 8-11). These findings underscore the crucial role of mechanical force and TiO<sub>2</sub> in facilitating the halogenation reaction. We also tested other oxides, including SiO<sub>2</sub>, carbon black and BaTiO<sub>3</sub> (Figure S1). Replacing TiO<sub>2</sub> with SiO<sub>2</sub> resulted in a slight decrease in the yield of benzyl chloride. In contrast, the use of BaTiO<sub>3</sub> or carbon black led to a more significant reduction in yield, indicating that surface acidity also plays a crucial role in the reaction. Therefore, our subsequent investigation was centered using TiO<sub>2</sub> (50 wt%) as tribo-catalyst with two ZrO<sub>2</sub> balls (10 mm) at 30 Hz. The gel permeation chromatography (GPC) was used to characterize the change of number-average molecular weight ( $M_n$ ) of PVC during ball milling. We observed a gradual decrease in  $M_n$  with the increase of TiO<sub>2</sub> content or milling frequency (Figure S2 and S3). Moreover, the use of large balls facilitated the degradation of PVC (Figure S4).

These results were consistent with the findings from the chlorination of benzyl alcohol. As shown in [Figure S2-S4](#), the higher molecular weight peak suggested the inter-chain coupling occurring during the ball milling process, particularly under conditions with a high yield of benzyl chloride. We conjecture that a greater extent of dehydrochlorination leads to a more unsaturated polymer structure for inter-chain coupling.

**Table 1. Optimization of the reaction conditions.** <sup>[a]</sup>



Entry	TiO <sub>2</sub> (wt%)	Frequency (Hz)	Ball		Yield (%) <sup>[b]</sup>
			Number	Size (mm)	
1	10	30	2	10	13
2	20	30	2	10	15
3	30	30	2	10	62
4	40	30	2	10	72
5	50	30	2	10	83
6	0	30	2	10	10
7	50	10	2	10	< 1
8	50	20	2	10	16
9	50	30	2	12	84
10	50	30	6	7	1
11	50	30	16	5	< 1

<sup>[a]</sup> Reaction conditions: PVC (200 mg, 3.2 mmol (based on the repeating unit)), benzyl alcohol (31  $\mu$ L, 0.3 mmol) and TiO<sub>2</sub> were charged inside a 10 mL ZrO<sub>2</sub> milling jar using two ZrO<sub>2</sub> ball (10 mm in diameter). The mixture was milled at 30 Hz for 3 h under air. <sup>[b]</sup> Determined by GC-MS with an internal standard curve.

With the optimized conditions in hand, we set to examine the kinetics of PVC degradation and benzyl alcohol chlorination. GC-MS data confirmed that the yield of benzyl chloride reached 95% after 4 h, without the formation of dibenzyl ether side product ([Figure 1a](#)). In contrast, the yield was significantly lower in the absence of TiO<sub>2</sub>. In addition, the proton nuclear magnetic resonance (<sup>1</sup>H NMR) spectra also confirmed a substantial amount of benzyl alcohol remains unreacted in the absence of TiO<sub>2</sub> ([Figure S5](#)). The internal temperature of the jar, measured using an infrared thermal camera, was determined to be 49.7 °C ([Figure S6](#)). This indicates that the chlorination of alcohols within the ball milling system occurs under mild conditions, obviating the necessity for elevated thermal condition (120°C), which helps to prevent the formation of side products. We speculated that TiO<sub>2</sub> functions not only as a tribo-catalyst but also as a Lewis acid to activate C-Cl bond. This mechanochemical activation is intrinsically linked to the degradation of PVC. We noted a continuous decreased in the *M<sub>n</sub>* of d-PVC under different milling time. Specifically, in the presence of TiO<sub>2</sub>, *M<sub>n</sub>* decreased from 65.0 kDa to 25.5 kDa, while the *M<sub>n</sub>* only decreased to 33.9 kDa without TiO<sub>2</sub> after 4 h of ball milling ([Figure 1b, c](#)). It appears that further degradation of PVC requires longer ball milling time, which will be discussed later in the paper.

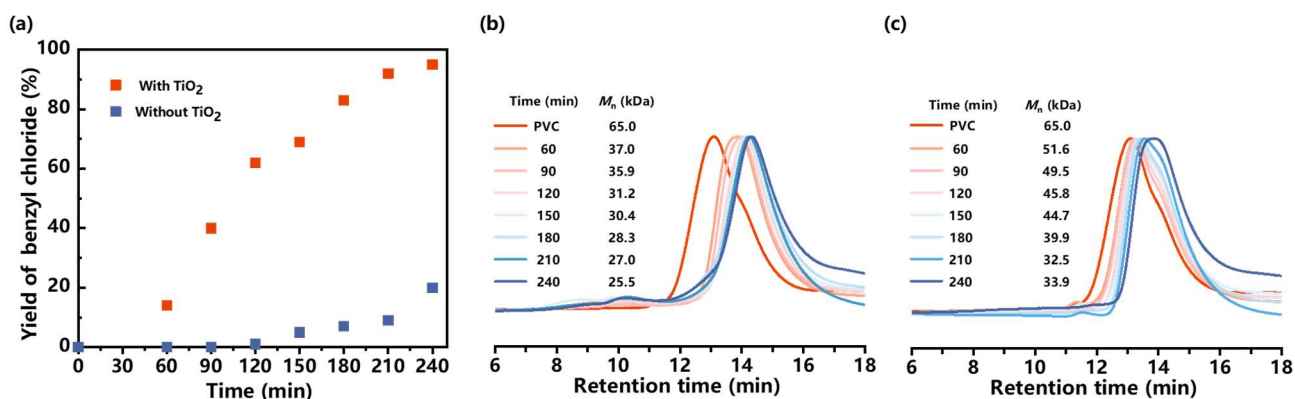


**Figure 1.** The benzyl alcohol chlorination and degradation of PVC at different milling time. (a) Yield of benzyl chloride with or without TiO<sub>2</sub>. (b)  $M_n$  of d-PVC with TiO<sub>2</sub> or (c) without TiO<sub>2</sub>.

To investigate the impact of ball milling on the tribo-catalyst, we performed structural characterizations of TiO<sub>2</sub> before and after the reaction. Scanning electron microscope (SEM) and transmission electron microscope (TEM) images confirmed the morphology of TiO<sub>2</sub> nanoparticles remained unchanged (Figure S7 and S8). The observed interplanar spacing of 0.35 nm corresponds to the (101) plane of anatase TiO<sub>2</sub>. This result aligns with the X-ray diffraction (XRD) analysis shown in Figure S9 (PDF #211272), suggesting that the crystal structure did not undergo significant changes during the reaction. The O1s spectra of the TiO<sub>2</sub> before and after reaction via X-ray photoelectron spectroscopy (XPS) analysis were listed in Figure S10. The oxygen species can be categorized into two components, lattice oxygen ( $\approx 530.0$  eV) and oxygen vacancies ( $\approx 531.7$  eV). Following mechanochemical treatment, an increase in oxygen vacancy content was observed on the surface of the TiO<sub>2</sub>, which may facilitate the catalytic electron transfer process.<sup>25,26</sup>

To investigate the substrate scope of this method, we examined a variety of aliphatic and benzylic alcohols. The yields of the target products were determined by <sup>1</sup>H NMR with terephthalaldehyde as an internal standard. The results are shown in Figure 2. Benzylic alcohols were efficiently converted into the desired products (1a and 1b) in 73-85% yields. However, the yield of 1c was lower due to the strong electron-withdrawing effect of the trifluoromethyl group. 2-Naphthalenemethanol gave the corresponding product 1d in a moderate yield of 70%. Primary aliphatic alcohols also afforded the expected chlorinated products with yields ranging from 66 to 85% (1i to 1l). Due to high activity of tertiary alcohol, the corresponding product was obtained in 81% yield (1f). We also examined the chlorination of cyclohexanol (1e) and 2,4-dichlorobenzyl alcohol (1h), achieving yields of 66% and 27%, respectively. These reactions are pivotal steps in the synthesis of diphenhydramine hydrochloride and lonidamine, two important pharmaceutical compounds. Interestingly, 1,2-benzenedimethanol preferentially underwent disubstitution, yielding 1h in 74%. In contrast, cyclohexane-1,4-diol favored monosubstitution to obtain 1m in 76% yield.

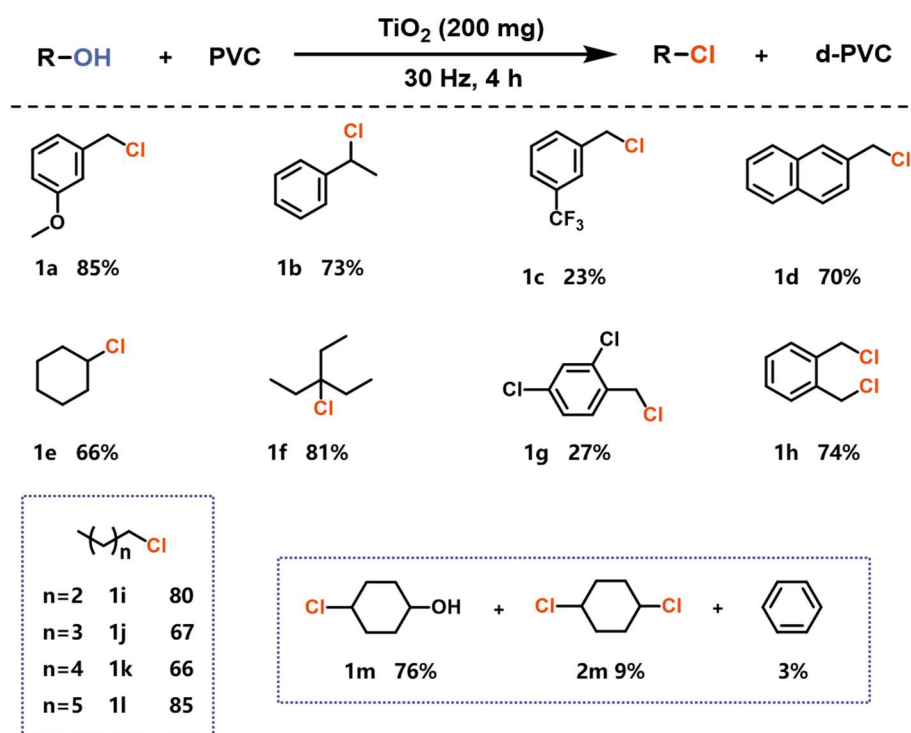


**Figure 2.** Substrate scope of chlorination reaction aliphatic and benzylic alcohols. Yields were determined by  $^1\text{H}$  NMR with terephthalaldehyde as internal standard.

Next, we estimated the degree of dechlorination by  $^1\text{H}$  NMR (see the SI for more details). After 4 h of ball milling, we achieved only 36% dehydrochlorination, a result consistent with the elemental analysis (31%) (Table S1). We opted to recycle and reuse PVC multiple times to maximize the utilization of residual chlorine. After each reaction cycle, we washed and dried the solid mixture in a vacuum oven at  $40^\circ\text{C}$ . Benzyl alcohol was then added for subsequent reaction under the same conditions. As shown in Figure 3a, the yield of benzyl chloride remained above 90% after the second cycle but gradually decreased in subsequent cycles. This decline in yield also aligns with the gradual reduction in residual chlorine content of PVC observed during the recycle experiments. During the degradation process, a trace amount of toluene was detected (Figure S11). We conjectured that intramolecular cyclization or intermolecular cross-linking reaction occurs from the conjugated polyene chain to form aromatic groups, which were decomposed into aromatic hydrocarbons.<sup>27,28</sup> We also employed GPC to track the  $M_n$  change of d-PVC throughout the dehydrochlorination process. As the number of cycles increased, the  $M_n$  of d-PVC exhibited a continuous decrease, ultimately reaching a value of 4.6 kDa after five cycles (Figure 3b).

To further analyze the structure of d-PVC, we conducted Fourier transform infrared (FT-IR) spectroscopy and NMR analysis. As depicted in Figure 3c, the IR signal of the C–Cl bond stretch at  $610\text{ cm}^{-1}$  gradually decreased, while the signal of the C=C bond stretch at  $1630\text{ cm}^{-1}$  and the C=O bond stretch at  $1710\text{ cm}^{-1}$  emerged. The appearance of C=O bond indicates that the oxidation reaction occurred during the degradation of PVC. As shown in Figure 3d, the  $^1\text{H}$  NMR signals corresponding to the -CHCl- of PVC (4.3–4.8 ppm) decreased with cycle experiments, while the characteristic peaks at 5.2–5.6 ppm and 7.0–7.9 ppm attributed to the protons of olefin group and aromatic group emerged. Besides the  $^1\text{H}$  NMR,  $^{13}\text{C}$  NMR analysis was performed to further identify the structure of d-PVC. In Figure 3e, the characteristic peaks at 125–127 ppm and 137 ppm confirmed the formation of olefin and aromatic group, and the peak at 155 ppm was attributed to carbonyl group.

To compare the thermal stability and decomposition behavior of PVC and d-PVC, the thermogravimetric analysis (TGA) was conducted (Figure 3f). Original PVC was found to be thermally stable up to 290 °C, after which it underwent dehydrochlorination in the temperature range of 290-350 °C. As the temperature increased from 400 to 700 °C, the polyene structures were gradually deconstructed and pyrolyzed into carbon. In contrast, the TGA curves of d-PVC exhibited a continuous mass loss over the temperature range of 100-500 °C, suggesting that the thermal stability of d-PVC is compromised due to the introduction of carbonyl structure during ball milling. After complete pyrolysis, it was found that d-PVC had a carbon yield of 30-40 wt%. It is worth noting that a small amount of insoluble polymer was observed after reaction (Figure S12). We selected the insoluble polymer from the last cycle to analyze its structure by solid-state cross-polarization magic-angle-spinning (CP-MAS) <sup>13</sup>C-NMR spectroscopy. Two new peaks appeared in the region of 110-130 ppm and 130-150 ppm, which were assigned to the olefin and aromatic structures. Simultaneously, the peak at 55 ppm, corresponding to the -C-Cl group, disappeared completely (Figure S13). However, the signal corresponded to the oxidized products (carbonyl group) was absent in the insoluble polymer.

This insoluble part can be used to prepare carbon materials by calcination in a tube furnace. The calcination was conducted at 700 °C for 3 h under N<sub>2</sub> atmosphere. After naturally cooled to room temperature, the carbon material was obtained for further characterization. In the Raman spectroscopy analysis, the peak at 1580 cm<sup>-1</sup> corresponds to the G peak, characteristic of graphitic carbon, while the D peak at 1350 cm<sup>-1</sup> is associated with disordered carbon (Figure S14). The intensity ratio of D and G peaks (I<sub>D</sub>/I<sub>G</sub>) was determined to be 0.9, indicating a moderate degree of graphitization. We also observed peaks in the range of 100-800 cm<sup>-1</sup> that are associated with residual TiO<sub>2</sub>. The TEM images suggested the carbon nanosheets were successfully generated through the calcination process. (Figure S15a, f-g). Besides, high-angle annular dark field scanning transmission electron microscopy (HAADFSTEM, Figure S15b) and corresponding energy-dispersive spectroscopy mappings (EDS; Figure S15c-e) showed the distribution of the elements of C, Ti, and O. Next, we investigated the photothermal behavior of carbon material in water using a thermometric indicator measure temperature as a function of NIR exposure time. The aqueous solution containing a 15 mg sample experienced a temperature increase of nearly 30°C after 10 min irradiation, while the temperature change in pure water was significantly lower. (Figure S16).



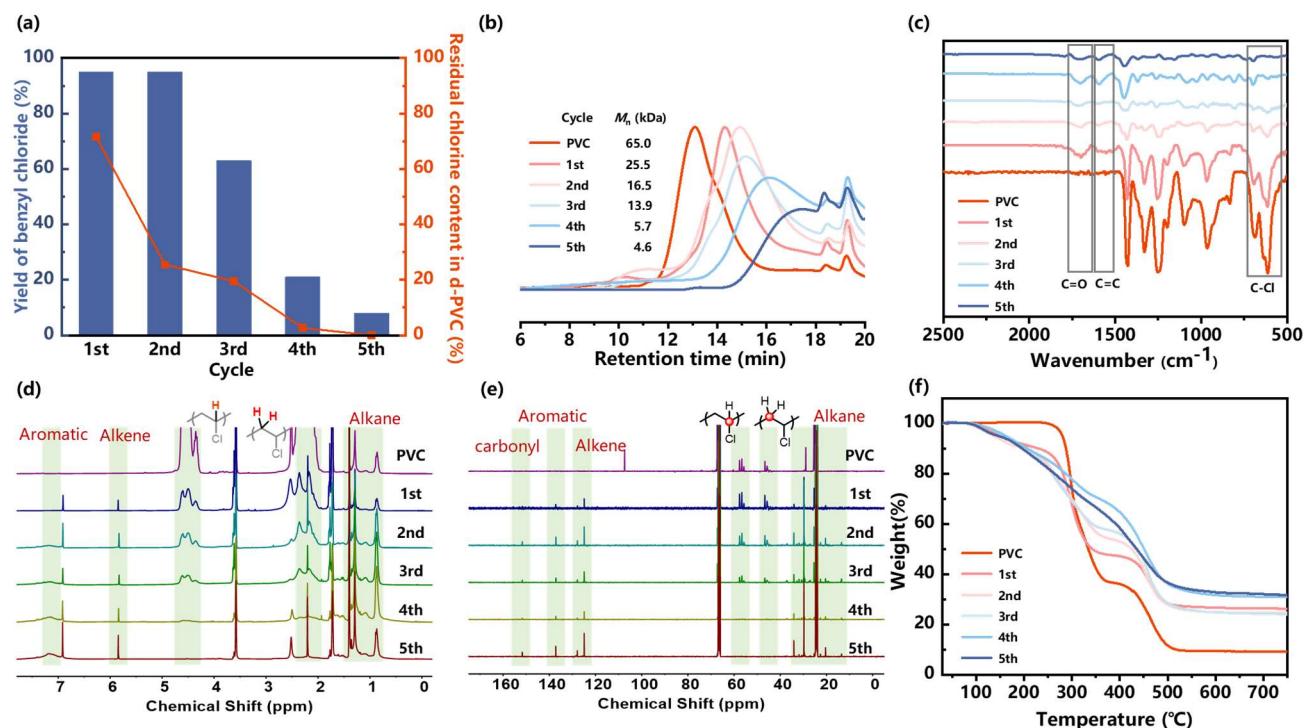


**Figure 3.** Experiments on the recycling and reusing of PVC. (a) Yield of benzyl chloride and residual chlorine content in d-PVC after each cycle. (b) GPC analysis of PVC and d-PVC after different cycle. (c) FT-IR curves of PVC and d-PVC after different cycle. (d) <sup>1</sup>H-NMR and (e) <sup>13</sup>C-NMR spectrum of PVC and d-PVC after different cycle. (f) TGA curves of PVC and d-PVC after each cycle.

To evaluate the applicability of this approach using real plastics, the commercial PVC storage bags were chopped into small pieces as chlorine source. During the ball milling process, the purple PVC bag pieces underwent direct dechlorination, resulting in the transformation into gray powder (Figure 4a). Unfortunately, a 39% yield of benzyl chloride was obtained, primarily due to the presence of various additives in PVC plastics. Therefore, we washed the pieces with ethanol to remove additives. Encouragingly, the mechanochemical chlorination of benzyl alcohol could be carried out effectively, achieving a benzyl chloride yield of 89%. To demonstrate the practical application of this method, we conducted a scale-up experiment of chlorination of 2-naphthalenemethanol in a 250 mL ZrO<sub>2</sub> ball-milling jar with planetary ball milling (550 rpm) (Figure 4b). The reaction time was extended to 12 h to accommodate the increased amounts of reactants. Upon completion of the reaction, an isolate yield of 57% was achieved. The high purity of the product was confirmed by <sup>1</sup>H NMR analysis.

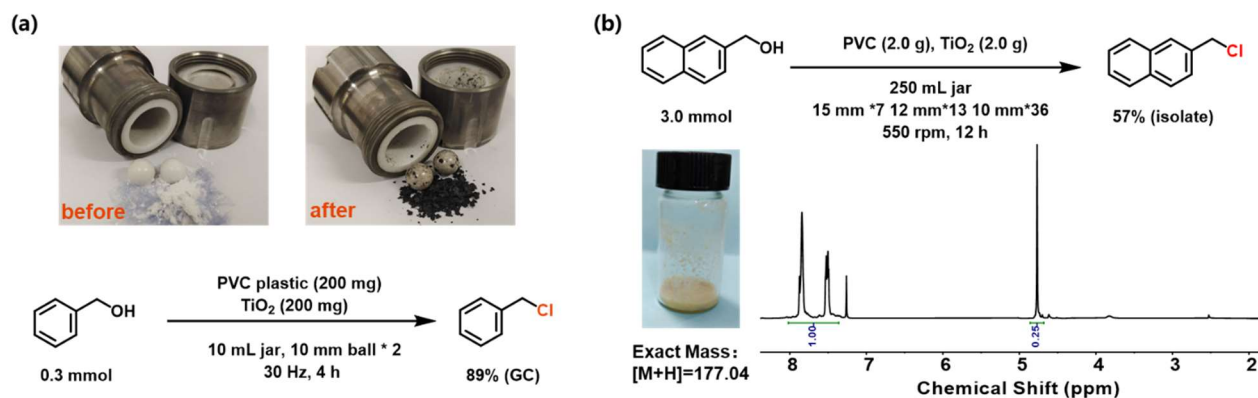


**Figure 4.** (a) Images of commercially available PVC products. (b) Scale-up experiment using planetary ball milling.

To gain insight into the mechanism, mechanistic studies were designed and performed. Previous work has demonstrated that strong bases facilitate the dehydrochlorination of PVC via an E2 pathway.<sup>19,20</sup> In our system, we conjectured that the C-Cl bond was activated via the single electron transfer (SET) mechanism to form free radical intermediate. We employed 2,2,6,6-tetramethylpiperidine 1-oxyl (TEMPO), a paramagnetic electron scavenger, to gain further insight into the mechanism of tribo-catalysis via electron paramagnetic resonance (EPR) spectroscopy. TEMPO would be reduced to TEMPOH in aqueous solution under the action of TiO<sub>2</sub>, resulting in a reduced EPR signal (Figure 6a). A control experiment without the catalyst showed no significant change in the EPR signal after ball milling. Subsequently, we used 1,3-dechlorobutane as a small molecule analogue of PVC to verify the carbon radical intermediate. When TEMPO was introduced into the reaction system of 1,3-dechlorobutane and TiO<sub>2</sub>, the TEMPO-trapped product was detected by GC-MS (Figure S17). These findings indicate that TiO<sub>2</sub> plays a crucial role in the generation of free radical intermediates through a tribo-catalytic mechanism. Next, we utilized 1,3-dechlorobutane as the Cl source together with TiO<sub>2</sub> for mechanochemical chlorination of benzyl alcohol. Following a 4 h ball milling reaction, benzyl chloride was obtained in a good yield of 83%.

Finally, density functional theory (DFT) was employed to evaluate the dissociation energy of the C-Cl bond under tribo-catalysis condition. Figures 6b show the tendency of the C-Cl bond breakage of 1,3,5-trichlorohexane compound, serving as a model molecule for PVC. The bond length of the C-Cl bond in PVC-like compound increased from 1.827 Å to 4.188 Å, suggesting its tendency for the formation of alkyl radicals. Based on the aforementioned results, a plausible SET mechanism of tribo-catalysis was proposed (Scheme 1). First, PVC undergoes dechlorination via a TiO<sub>2</sub> mediated SET pathway, resulting in the formation of carbon radical intermediate. Subsequently, the β-hydrogen atom from the carbon radical is eliminated, leading to the formation of C=C bond and HCl. Concurrently, benzyl alcohol reacts with HCl to yield benzyl chloride.



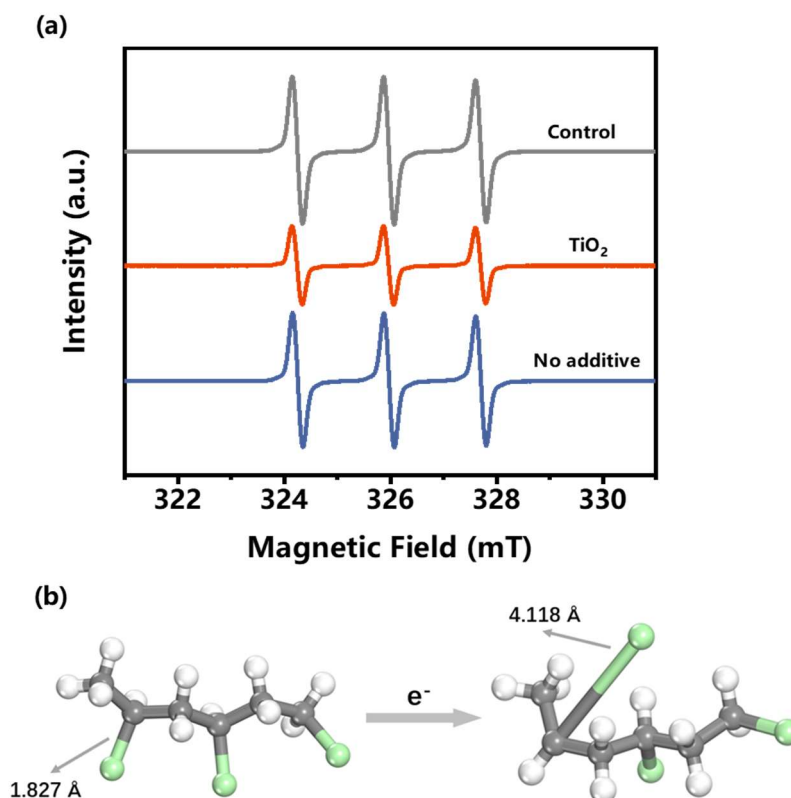
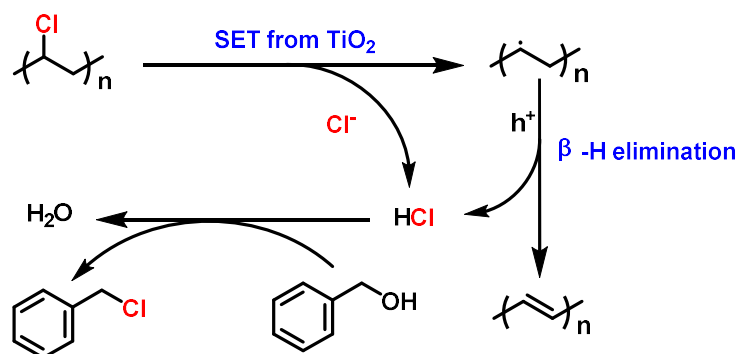


**Figure 5.** (a) Detection of TEMPO by EPR spectroscopy for various conditions. (b) The tendency of the C-Cl bond breakage of 1,3,5-trichlorohexane compound by DFT calculation.



**Scheme 1.** Possible mechanism of dehydrochlorination of PVC and chlorination of benzyl alcohol

In summary, we have developed an environment-friendly and sustainable method for the efficient halogenation of alcohols using waste PVC and tribo-catalyst. This approach enables the production of benzyl chloride with a high yield of 95% under solvent-free conditions. This method could be used for various aliphatic and benzylic alcohols. Cl can be completely removed after recycling and reusing of PVC. The NMR and FTIR analysis confirmed the dehydrochlorination of PVC, which contains olefin, carbonyl and aromatic structures. We demonstrated that the mechanochemical approach remains effective in real plastics, achieving an 89% yield of benzyl chloride. The scale-up experiments conducted using planetary ball milling yielded 2-(chloromethyl)naphthalene with an isolated yield of 57% on a 2g scale. Furthermore, experimental results together with DFT calculations verified that the dehydrochlorination of PVC involves SET mechanisms in this

study. These findings highlight the potential of mechanochemical treatment of waste PVC for sustainable chemical transformations.

## ASSOCIATED CONTENT

All experimental and characterization details are available in the Supporting Information.

## CONFLICTS OF INTEREST

There are no conflicts to declare.

## ACKNOWLEDGMENTS

This work was supported by the National Natural Science Foundation of China (22471185 and 22101195), Natural Science Foundation of Jiangsu Province (BK20210732), Science and Technology Pro-gram of Suzhou (ZXL2022480), the Priority Academic Program Development of Jiangsu Higher Education Institutions (PAPD), and the Program of Innovative Research Team of Soochow University.

## REFERENCES

- (1) Geyer, R.; Jambeck, J. R.; Law, K. L. Production, Use, and Fate of All Plastics Ever Made. *Sci. Adv.* **2017**, *3* (7), e1700782. <https://doi.org/10.1126/sciadv.1700782>.
- (2) Lu, L.; Li, W.; Cheng, Y.; Liu, M. Chemical Recycling Technologies for PVC Waste and PVC-Containing Plastic Waste: A Review. *Waste Manage.*, **2023**, *166*, 245–258. <https://doi.org/10.1016/j.wasman.2023.05.012>.
- (3) Zhang, S.; Han, H.; Cao, M.; Xie, Y.; Chen, J. Upvaluing Chlorinated Plastic Wastes. *Interdisciplinary Materials* **2024**, idm2.12211. <https://doi.org/10.1002/idm2.12211>.
- (4) Kots, P. A.; Vance, B. C.; Quinn, C. M.; Wang, C.; Vlachos, D. G. A Two-Stage Strategy for Upcycling Chlorine-Contaminated Plastic Waste. *Nat Sustain* **2023**, *6* (10), 1258–1267. <https://doi.org/10.1038/s41893-023-01147-z>.
- (5) Chu, M.; Liu, Y.; Lou, X.; Zhang, Q.; Chen, J. Rational Design of Chemical Catalysis for Plastic Recycling. *ACS Catal.* **2022**, *12* (8), 4659–4679. <https://doi.org/10.1021/acscatal.2c01286>.
- (6) O'Rourke, G.; Hennebel, T.; Stalpaert, M.; Skorynina, A.; Bugaev, A.; Janssens, K.; Van Emelen, L.; Lemmens, V.; De Oliveira Silva, R.; Colemonts, C.; Gabriels, P.; Sakellariou, D.; De Vos, D. Catalytic Tandem Dehydrochlorination–Hydrogenation of PVC towards Valorisation of Chlorinated Plastic Waste. *Chem. Sci.* **2023**, *14* (16), 4401–4412. <https://doi.org/10.1039/D3SC00945A>.
- (7) Bush, N. G.; Assefa, M. K.; Bac, S.; Mallikarjun Sharada, S.; Fieser, M. E. Controlling Selectivity for Dechlorination of Poly(Vinyl Chloride) with (Xantphos)RhCl. *Mater. Horiz.* **2023**, *10* (6), 2047–2052. <https://doi.org/10.1039/D2MH01293F>.
- (8) Liu, M.; Wu, X.; Dyson, P. J. Tandem Catalysis Enables Chlorine-Containing Waste as Chlorination Reagents. *Nat. Chem.* **2024**, *16*, 700–708. <https://doi.org/10.1038/s41557-024-01462-8>.
- (9) Fagnani, D. E.; Kim, D.; Camarero, S. I.; Alfaro, J. F.; McNeil, A. J. Using Waste Poly(Vinyl Chloride) to Synthesize Chloroarenes by Plasticizer-Mediated Electro(de)Chlorination. *Nat. Chem.* **2023**, *15*, 222–229. <https://doi.org/10.1038/s41557-022-01078-w>.
- (10) Feng, B.; Jing, Y.; Liu, X.; Guo, Y.; Wang, Y. Waste PVC Upcycling: Transferring Unmanageable Cl Species into Value-Added Cl-Containing Chemicals. *Appl. Catal. B: Environ.*, **2023**, *331*, 122671. <https://doi.org/10.1016/j.apcatb.2023.122671>.

- (11)Liu, H. Repurposing of Halogenated Organic Pollutants via Alkyl Bromide-Catalysed Transfer Chlorination. *Nat. Chem.* **2024**, *16*, 1505–1514.
- (12)Cao, R.; Zhang, M.-Q.; Jiao, Y.; Li, Y.; Sun, B.; Xiao, D.; Wang, M.; Ma, D. Co-Upcycling of Polyvinyl Chloride and Polyesters. *Nat Sustain* **2023**, *6*, 1685–1692. <https://doi.org/10.1038/s41893-023-01234-1>.
- (13)Lee, H. W.; Yoo, K.; Borchardt, L.; Kim, J. G. Chemical Recycling of Polycarbonate and Polyester without Solvent and Catalyst: Mechanochemical Methanolysis. *Green Chem.* **2024**, *26* (4), 2087–2093. <https://doi.org/10.1039/D3GC03643J>.
- (14)Tricker, A. W.; Osibo, A. A.; Chang, Y.; Kang, J. X.; Ganesan, A.; Anglou, E.; Boukouvala, F.; Nair, S.; Jones, C. W.; Sievers, C. Stages and Kinetics of Mechanochemical Depolymerization of Poly(Ethylene Terephthalate) with Sodium Hydroxide. *ACS Sustainable Chem. Eng.* **2022**, *10* (34), 11338–11347. <https://doi.org/10.1021/acssuschemeng.2c03376>.
- (15)Hergesell, A. H.; Baarslag, R. J.; Seitzinger, C. L.; Meena, R.; Schara, P.; Tomović, Ž.; Li, G.; Weckhuysen, B. M.; Vollmer, I. Surface-Activated Mechano-Catalysis for Ambient Conversion of Plastic Waste. *J. Am. Chem. Soc.* **2024**, *146* (38), 26139–26147. <https://doi.org/10.1021/jacs.4c07157>.
- (16)Nguyen, V. S.; Chang, Y.; Phillips, E. V.; DeWitt, J. A.; Sievers, C. Mechanocatalytic Oxidative Cracking of Poly(Ethylene) Via a Heterogeneous Fenton Process. *ACS Sustainable Chem. Eng.* **2023**, *11* (20), 7617–7623. <https://doi.org/10.1021/acssuschemeng.3c01054>.
- (17)Inoue, T.; Miyazaki, M.; Kamitani, M.; Kano, J.; Saito, F. Dechlorination of Polyvinyl Chloride by Its Grinding with KOH and NaOH. *Adv. Powder. Technol.*, **2005**, *16* (1), 27–34. <https://doi.org/10.1163/1568552053166638>.
- (18)Xiao, X.; Zeng, Z.; Xiao, S. Behavior and Products of Mechano-Chemical Dechlorination of Polyvinyl Chloride and Poly (Vinylidene Chloride). *J Hazard Mater.*, **2008**, *151* (1), 118–124. <https://doi.org/10.1016/j.jhazmat.2007.05.067>.
- (19)Lu, J.; Borjigin, S.; Kumagai, S.; Kameda, T.; Saito, Y.; Yoshioka, T. Practical Dechlorination of Polyvinyl Chloride Wastes in NaOH/Ethylene Glycol Using an up-Scale Ball Mill Reactor and Validation by Discrete Element Method Simulations. *Waste. Manage.*, **2019**, *99*, 31–41. <https://doi.org/10.1016/j.wasman.2019.08.034>.
- (20)Choudhury, N.; Kim, A.; Kim, M.; Kim, B. Mechanochemical Degradation of Poly(Vinyl Chloride) into Non-Toxic Water-Soluble Products via Sequential Dechlorination, Heterolytic Oxirane Ring-Opening, and Hydrolysis. *Adv. Mater.* **2023**, *35*, 2304113. <https://doi.org/10.1002/adma.202304113>.
- (21)Li, X.; Tong, W.; Shi, J.; Chen, Y.; Zhang, Y.; An, Q. Tribocatalysis Mechanisms: Electron Transfer and Transition. *J. Mater. Chem. A* **2023**, *11* (9), 4458–4472. <https://doi.org/10.1039/D2TA08105A>.
- (22)Wu, M. Regulation of Friction Pair to Promote Conversion of Mechanical Energy to Chemical Energy on Bi<sub>2</sub>WO<sub>6</sub> and Realization of Enhanced Tribocatalytic Activity to Degrade Different Pollutants. *J Hazard Mater.*, **2023**, *459*, 132147.
- (23)Tang, Q.; Zhu, M.; Zhang, H.; Gao, J.; Kwok, K. W.; Kong, L.-B.; Jia, Y.; Liu, L.; Peng, B. Enhanced Tribocatalytic Degradation of Dye Pollutants through Governing the Charge Accumulations on the Surface of Ferroelectric Barium Zirconium Titanate Particles. *Nano Energy* **2022**, *100*, 107519. <https://doi.org/10.1016/j.nanoen.2022.107519>.
- (24)Lei, H. Tribo-Catalytic Degradation of Organic Pollutants through Bismuth Oxyiodate Triboelectrically Harvesting Mechanical Energy. *Nano Energy* **2020**, *78*, 105290.
- (25)Luo, X.; Xu, L.; Yang, L.; Zhao, J.; Asefa, T.; Qiu, R.; Huang, Z. Ball Milling of La<sub>2</sub>O<sub>3</sub> Tailors the Crystal Structure, Reactive Oxygen Species, and Free Radical and Non-Free Radical Photocatalytic Pathways. *ACS Appl. Mater. Interfaces* **2024**, *16* (15), 18671–18685.

<https://doi.org/10.1021/acsami.3c15677>.

- (26) Yang, Y.; Zhang, S.; Wang, S.; Zhang, K.; Wang, H.; Huang, J.; Deng, S.; Wang, B.; Wang, Y.; Yu, G. Ball Milling Synthesized MnO<sub>x</sub> as Highly Active Catalyst for Gaseous POPs Removal: Significance of Mechanochemically Induced Oxygen Vacancies. *Environ. Sci. Technol.* **2015**, *49* (7), 4473–4480. <https://doi.org/10.1021/es505232f>.
- (27) Feng, B.; Guo, Y.; Liu, X.; Wang, Y. Transforming PVC Plastic Waste to Benzene via Hydrothermal Treatment in a Multi-Phase System. *Green Chem.* **2023**, 10.1039.D3GC03063F. <https://doi.org/10.1039/D3GC03063F>.
- (28) Dong, N.; Hui, H.; Li, S.; Du, L. Study on Preparation of Aromatic-Rich Oil by Thermal Dechlorination and Fast Pyrolysis of PVC. *J Anal Appl Pyrol.* **2023**, *169*, 105817. <https://doi.org/10.1016/j.jaap.2022.105817>.